problem of sex chromosome degeneration has been to extend the *msl*-based mechanism. This has occurred despite the fact that, on an evolutionary time scale, the requirements for compensation appear gradually, gene by gene. These results suggest that the extant compensatory system is adopted when new requirements for dosage compensation arise. The constraints on developing new dosage compensation mechanisms probably derive from the difficulty in evolving systems able sex-specifically to regulate functionally unrelated genes, which have in common only the fact that they reside on the same chromosome. Taking all these considerations together, we expect to find identical mechanisms functioning in phylogenetically very distant species.

Note added in proof: Histone H4 acetylated at lysine residue 16, known to be implicated in the hypertranscription mechanism in *D. melanogaster*, is also enriched in the newly evolved X chromosomes of *D. pseudoobscura* and *D. miranda*[17]. □

Methods

Antibodies. We have used rat polyclonal antibodies against three of the MSLs (MSL-1, amino acids 618–939; MSL-2, 534–669 (ref. 5); and MSL-3, 324–513 (ref. 15)). These antibodies were selected on the basis of results of preliminary experiments using *Drosophila pseudoobscura*, *D. virilis* and *Chymomyza procnemis*. Only these antibodies stained the male X chromosomes of at least one of these species. Six other antibodies, including two raised against MLE, gave negative results. The results summarized in Fig. 1 are based on at least two preparations for each combination of antibody, sex and species. The negative assessments for *Scaptodrosophila lebanonensis* and *Drosophila busckii* males are based on at least 5 chromosome preparations per antibody. The number of epitopes recognized in distant species is probably small because: (1) none of the antibodies is positive in all the species; (2) positive signals do not strictly correlate with the phylogenetic proximity to *D. melanogaster*; and (3) signal intensity in other species is lower than in *D. melanogaster*. Therefore, the simplest explanation for the failure to observe binding in those two species is that they have lost the conserved epitope(s) recognized by our antibodies.

Immunostainings. Third instar larvae were sexed according to the size of their gonads. Sex was verified by observation of polytene chromosomes from the salivary glands. Under phase contrast optics, males showed one to three pale arms, depending on the species. Moreover, in some cases the male X chromosome had a peculiar shape, was shorter or seemed diffuse when compared with the autosomes. When possible, it was further determined that the stained chromosome(s) corresponded to the X chromosome(s) by comparison with the available chromosome maps. Immunostainings were performed as described in ref. 5. Antibodies were generally used at the same dilution routinely chosen for *D. melanogaster* (1:50). Although at this concentration the intensity of staining observed in the other species was substantially lower than in *D. melanogaster*, the male X chromosome was easily visualized in every preparation of most species. Only in *D. pseudoobscura*, *D. miranda* and *Hirtodrosophila pictiventris* was the fluorescence level so low that in some slides the X chromosome was not easily distinguishable. In these species, higher concentrations (up to 1:20) were used. DAPI was used to stain the chromosomes for localization and study under fluorescence optics.

Received 1 May; accepted 7 August 1996.

1. Charlesworth, B. *Science* **251,** 1030–1033 (1991).
2. Charlesworth, B. *Curr. Biol.* **6,** 149–162 (1996).
3. Bull, J. J. *Evolution of Sex Determining Mechanisms* (Benjamin/Cummings, 1983).
4. Baker, B. S., Gorman, M. & Marín, I. *Annu. Rev. Genet.* **28,** 491–521 (1994).
5. Bashaw, G. J. & Baker, B. S. *Development* **121,** 3245–3258 (1995).
6. Zhou, S. *et al. EMBO J.* **14,** 2884–2895 (1996).
7. Kelley, R. L. *et al. Cell* **81,** 867–877 (1995).
8. Grimaldi, D. A. *Bull. Am. Mus. Nat. His.* **197,** 1–139 (1990).
9. Russo, C. A. M., Takezaki, N. & Nei, M. *Mol. Biol. Evol.* **12,** 391–404 (1995).
10. Beverley, S. M. & Wilson, A. C. *J. Mol. Evol.* **21,** 1–13 (1984).
11. Kwiatowski, J., Skarecky, D., Bailey, K. & Ayala, F. J. *J. Mol. Evol.* **38,** 443–454 (1994).
12. Abraham, I. & Lucchesi, J. C. *Genetics* **78,** 119–126 (1974).
13. Strobel, E., Pelling, C. & Arnheim, N. *Proc. Natl Acad. Sci. USA* **75,** 931–935 (1978).
14. Das, M., Mutsuddi, D., Duttagupta, A. K. & Mukherjee, A. S. *Chromosoma* **87,** 373–388 (1982).
15. Gorman, M., Franke, A. & Baker, B. S. *Development* **121,** 463–475 (1995).
16. Dobzhansky, T. *Genetics* **20,** 377–391 (1935).
17. Steinemann, M., Steinemann, S. & Turner, B. M. *Chromosome Res.* **4,** 185–190 (1996).

ACKNOWLEDGEMENTS. We thank D. A. Grimaldi for his advice concerning drosophilid phylogeny; G. Bohm for preparation of fly food; and the National *Drosophila* Species Resource Center (Bowling Green, Ohio and the European *Drosophila* Stock Centre (Umea, Sweden) for *Drosophila* stocks. This work was supported by a postdoctoral fellowship (Ministerio de Educación y Ciencia, Spain) to I.M., an NIH predoctoral training grant to G.J.B. and an NIH grant to B.S.B.

CORRESPONDENCE and requests for materials should be addressed to I.M. (e-mail: marin@cmgm.stanford.edu).

Functional neuroanatomy of human rapid-eye-movement sleep and dreaming

Pierre Maquet*†, Jean-Marie Péters*, Joël Aerts*, Guy Delfiore*, Christian Degueldre*, André Luxen* & Georges Franck*†

* Cyclotron Research Centre (B30), University of Liège, 4000 Liège, Belgium
† Department of Neurology, CHU Sart Tilman (B35), 4000 Liège, Belgium

RAPID-EYE-MOVEMENT (REM) sleep is associated with intense neuronal activity, ocular saccades, muscular atonia and dreaming[1,2]. The function of REM sleep remains elusive and its neural correlates have not been characterized precisely in man. Here we use positron emission tomography and statistical parametric mapping to study the brain state associated with REM sleep in humans. We report a group study of seven subjects who maintained steady REM sleep during brain scanning and recalled dreams upon awakening. The results show that regional cerebral blood flow is positively correlated with REM sleep in pontine tegmentum, left thalamus, both amygdaloid complexes, anterior cingulate cortex and right parietal operculum. Negative correlations between regional cerebral blood flow and REM sleep are observed bilaterally, in a vast area of dorsolateral prefrontal cortex, in parietal cortex (supramarginal gyrus) as well as in posterior cingulate cortex and precuneus. Given the role of the amygdaloid complexes in the acquisition of emotionally influenced memories, the pattern of activation in the amygdala and the cortical areas provides a biological basis for the processing of some types of memory during REM sleep.

Thirty young, healthy, right-handed male subjects (mean age, 22.5 years; range, 20–25) participated in this study, which took place over 3 polygraphically monitored nights spent on a scanner couch, at one-week intervals. Polygraphic recordings included electroencephalogram (recorded between electrode pairs C3–A2 and C4–A1), EOG (electro-oculogram) and chin EMG (electromyogram), and were scored using the criteria of ref. 3. Subjects were asked not to sleep during the night preceding the second and third test nights to ensure optimal sleep stability despite difficult experimental conditions (head stabilized using a face mask secured to the scanner head holder and left arm cannulated and immobilized). Subjects were selected if they could maintain two periods of slow-wave sleep and of REM sleep (20 min each) during the first two test nights. Nineteen subjects were finally selected.

During the third test night, regional cerebral blood flow (rCBF) distribution was recorded as an index of neuronal activity using six slow intravenous infusions of $H_2{}^{15}O$ scheduled during the following states: wakefulness, slow-wave sleep, slow-wave sleep, REM sleep, REM sleep, wakefulness. This order was imposed by the physiological preponderance of slow-wave sleep early in the night and of REM sleep in the early morning. During sleep, scans were done when polysomnography showed characteristic sleep patterns (slow-wave or REM sleep) that remained stable over the 5-min period necessary for water production. After each sleep scan, the subjects were woken up and asked to describe what was in their minds. Dream reports were scored following the classification system of ref. 4. Four subjects were studied during a complete set of states (2 wakeful, 2 slow-wave, 2 REM sleep states); another group of three subjects was scanned during 2 wakeful and 2 REM sleep states but changed their sleep stage during the injections in the slow-wave sleep state. All subjects recalled a dream after awakening from REM sleep. The dream contents included various settings, characters, objects and activities. A final group of four subjects were scanned during 2 wakeful and 2 slow-wave sleep

states but changed their sleep stage during the injections in the REM sleep stage. The analysis was done using these three groups (11 subjects total, 7 with stable REM sleep). Positron emission tomography (PET) data were analysed using statistical parametric mapping. Correlations between rCBF and the presence of REM sleep were assessed (see Fig. 1 legend), to identify brain areas whose activity was associated with REM sleep.

Significant positive correlations between rCBF and REM sleep (Table 1 and Fig. 1) were observed in the anterior cingulate cortex (mainly Brodmann's area (BA) 24), the posterior part of the right parietal operculum (anterior part of BA 40), the right amygdala and surrounding entorhinal cortex, and in a region encompassing the left amygdala and surrounding entorhinal cortex, the thalamic nuclei, the dorsal mesencephalon and pontine tegmentum. Within this area, local maxima of blood flow were located in the left amygdala, left thalamus and pontine tegmentum. Significant negative correlations between rCBF and REM sleep (Table 2 and Fig. 2) were found in precuneus and adjacent posterior cingulate cortex (BA 31) and, bilaterally, in a large area of dorsolateral prefrontal cortex (mainly BA 10, but also 46, 9, 8 and the lateral part of BA 11) and in parietal cortex (supramarginal gyrus, BA 40).

These results provide the first comprehensive description of the distribution of cerebral activity during REM sleep in man. They confirm previous PET data suggesting a metabolic activation of the brainstem[5], the limbic system[6] and the cingulate cortex[7] during REM sleep. Recently, a positive correlation was reported between cerebral glucose metabolism and ocular saccades during REM sleep in regions where we report a negative correlation between rCBF and REM sleep (prefrontal and parietal areas)[8]. The results do not necessarily conflict with ours because the different variables characterized two different neural networks.

REM sleep is generated by nuclei of the mesopontine reticular formation[1,9]. These nuclei are an important source of activation of thalamic nuclei which, in turn, activate the cortical mantle[9]. The significant correlation between rCBF and REM sleep observed in pontine tegmentum and thalamic nuclei most probably reflects the activation of these central-core structures during REM sleep. The left-sided predominance of the thalamic activation may be due to a statistical bias of the sampled population, or may reflect true lateralization of thalamic activation in right-handed subjects.

Our results show that the intense and widespread cortical activation during REM sleep is not uniform: several regions are more, and others are less, active than the rest of the brain. The significant correlation found in the amygdala is conspicuous. The role of the amygdaloid complexes in REM sleep phenomenology, although suggested in animals[11], has never been explicitly demonstrated in humans. The amygdaloid complexes receive an important set of afferent nerve connections arising from the dorsal pons[12] and intralaminar thalamic nuclei[13], by which they could be activated during REM sleep. On the other hand, the amygdaloid complexes project back to subcortical structures (hypothalamus and several brainstem nuclei)[12]. By these subcortical projections, the amygdaloid complexes could induce the autonomic manifestations that are commonly observed during REM sleep[15].

The amygdaloid complexes also have reciprocal connections with many cortical areas[12,16], which enable the amygdala to establish cross-modal sensory-affective associations[12,16,17]. The amygdaloid complexes are also implicated in the formation and consolidation of memories paired with emotional stimuli[12,16], by regulating the storage of long-term memory in other cerebral regions[18]. Periods of REM sleep have also been implicated in the consolidation of memory traces[19]. In man, REM sleep particularly influences the processing of 'procedural–implicit' memory[19] and also of memories acquired under emotionally charged conditions[20].

TABLE 1 Increased brain activity during REM sleep

Area (Brodmann's area)	*x*	*y*	*z*	*Z* score	*P* (corrected)
Anterior cingulate cortex (24)	2	8	36	5.15	0.001
	0	−12	44	4.47	0.010
Right parietal operculum (40)	60	−22	16	4.88	0.002
Right amygdaloid complex	16	−4	−12	4.29	0.021
Left amygdaloid complex	−18	−6	−12	5.15	0.001
Left thalamus	−10	−22	4	4.05	0.049
Pons	−6	−34	−28	4.21	0.028

Localization and statistical results concerning the local maxima of the brain areas where the activity is positively correlated with REM sleep. Coordinates are defined in the sterotactic space of Talairach[28], relative to anterior commissure. *x* represents the lateral distance from midline (positive, right); *y* is the anteroposterior distance from anterior commissure (positive: anterior); *z* represents the rostrocaudal distance from the bicommissural plane (positive: rostral). The areas are significantly correlated at a threshold of $P = 0.001$, by reference to unit normal distribution ($Z = 3.09$), and at a threshold of corrected $P < 0.05$ (corrected *P*, the probability that the rCBF variation could have occurred by chance over the entire volume analysed).

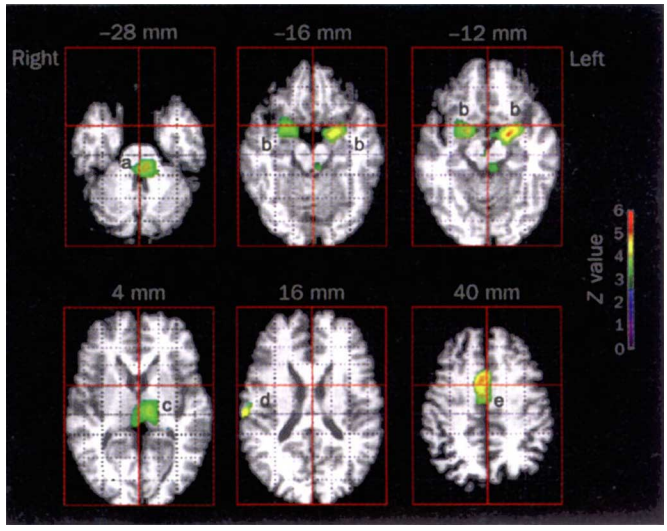

FIG. 1 Transverse sections showing brain areas where activity showed a significant positive correlation with REM sleep. Functional PET results are displayed at threshold of $Z = 3.09$ ($P < 0.001$), and superimposed, for anatomical reference, upon a T1-weighted magnetic resonance imaging scan normalized into the Talairach space[28]. Section numbers refer to the distance from bicommissural plane. a, pons; b, amygdaloid complexes; c, thalamus; d, right parietal operculum; e, anterior cingulate cortex.
METHODS. PET acquisitions were obtained with a Siemens CTI 951 scanner in 2D mode. For each subject, six 120-s scans were made using $H_2{}^{15}O$ infusion technique, under continuous polygraphic monitoring. PET data were corrected for attenuation and background activity, and reconstructed with a Hanning filter (cutoff frequency, 0.5 cycles per pixel; 8.7 mm FWHM (full width at half-maximum)). Data were processed using the statistical parametric mapping software. Individual data were realigned[28], normalized into stereotactic space[28] then smoothed with a 12-mm FWHM gaussian filter. A design matrix was specified, which included global activity as confounding covariate[29]. This matrix allowed for an across-group analysis looking for regionally specific condition effects. The analysis identified the brain regions where rCBF was significantly correlated with the presence of a particular functional state (such as REM sleep), using linear contrasts (+1 or −1 for REM sleep scans, 0 for slow-wave sleep and wakeful-state scans). The resulting maps (SPM{*t*}) were transformed to the unit normal distribution (SPM{*Z*}) and thresholded at $P < 0.001$ ($Z = 3.09$). The resulting foci of activation were characterized in terms of the probability that the peak height could have occurred by chance over the entire volume analysed (corrected *P* value ≤ 0.05). Details of the wakeful and slow-wave sleep states will be published elsewhere.

Thus, the activation of the amygdaloid complexes suggests that REM sleep contributes to some memory processing. Moreover, the rCBF distribution suggests a functional link between the amygdala, the hippocampal formations and cortical areas during REM sleep. First, the anterior part of the entorhinal cortex is embedded within the activation foci centred on the amygdaloid complexes. As they have dense reciprocal connections with the entorhinal cortex[12], their coactivation is possible. Second, the anterior cingulate cortex to which the amygdaloid complexes send their largest cortical efferent projection[12], is also significantly correlated with REM sleep. Third, a significant correlation is found in the right parietal operculum. Although this activation might be due to a statistical bias of the sampled population, we feel that it corresponds to an actual asymmetrical activation. In non-human primates, this area is the only somatosensory region that receives amygdalar projections[16]. Its activation might reflect the processing of the somaesthesic stimulations, common to all our subjects, coming from the cannulation and immobilization of their left arm.

Other cortical areas receive abundant amygdalar projections (medial orbitofrontal, temporal, occipital and insular cortices)[12,16]. The activation of occipital[8,21] and temporal[5] areas during REM sleep have been suggested by previous neuroimaging studies in humans. Here, none of these regions were significantly correlated with REM sleep, probably because the group analysis averaged out cortical activations specific to each individual subject or even to each scanned REM sleep episode.

A further indication of amygdalocortical interplay during REM sleep is, that the regions which are negatively correlated with REM sleep are known to receive few or no amygdalar efferents[12,16,22,23], and consequently, are not likely to be activated during REM sleep as much as cortical areas characterized by high amygdalar input. Dorsolateral prefrontal areas and precuneus have been shown to participate in the encoding and retrieval of episodic memory[24], whereas inferior parietal lobules (and prefrontal areas) participate in working memory[25,26]. Our results suggest that these memory processes are not prominent during REM sleep.

In summary, there are indications that during REM sleep, functional interactions occur between the amygdaloid complexes, anterior cingulate cortex and various, mainly posterior, areas. These interactions might lead to the reactivation of affective components of memories, thereby bringing about the consolidation of memory traces.

As all our subjects recalled a dream after REM sleep scans, the distribution of rCBF may reflect their dreaming activity. The amygdalo[12,16] cingulate[27] coactivation could account for the emotional and affective aspects of dreams. Other formal char-

TABLE 2 Decreases in brain activity during REM sleep

Area (Brodmann's area)		x	y	z	Z score	P (corrected)
Right dorsolateral prefrontal cortex	(10)	22	56	−4	6.36	<0.001
		36	48	0	5.86	<0.001
		26	48	16	5.07	0.001
		26	40	20	4.81	0.003
	(11)	18	42	−12	4.34	0.017
		22	30	−16	4.19	0.029
	(9)	20	38	36	4.78	0.003
	(46)	40	16	24	4.22	0.026
	(8)	28	10	48	5.32	<0.001
Left dorsolateral prefrontal cortex	(10)	−20	44	−8	5.10	0.001
		−34	48	−4	4.80	0.003
		−26	54	4	4.62	0.006
		−10	62	16	4.53	0.008
		−16	56	−4	4.47	0.010
		−16	62	8	4.44	0.012
	(11)	−12	36	−16	4.94	0.001
	(46)	−32	44	16	5.27	<0.001
	(47)	−34	40	−8	5.16	<0.001
Right parietal cortex	(40)	48	−46	36	5.51	<0.001
		40	−68	36	4.45	0.011
Left parietal cortex	(40)	−44	−50	36	4.07	0.047
Precuneus and		8	−64	28	4.80	0.003
posterior cingulate cortex	(31)	16	−66	32	4.73	0.004
		2	−42	32	4.48	0.010

Localization and statistical results concerning the local maxima of the brain areas where the activity is negatively correlated with REM sleep. Coordinates and correlations are determined as for Table 1.

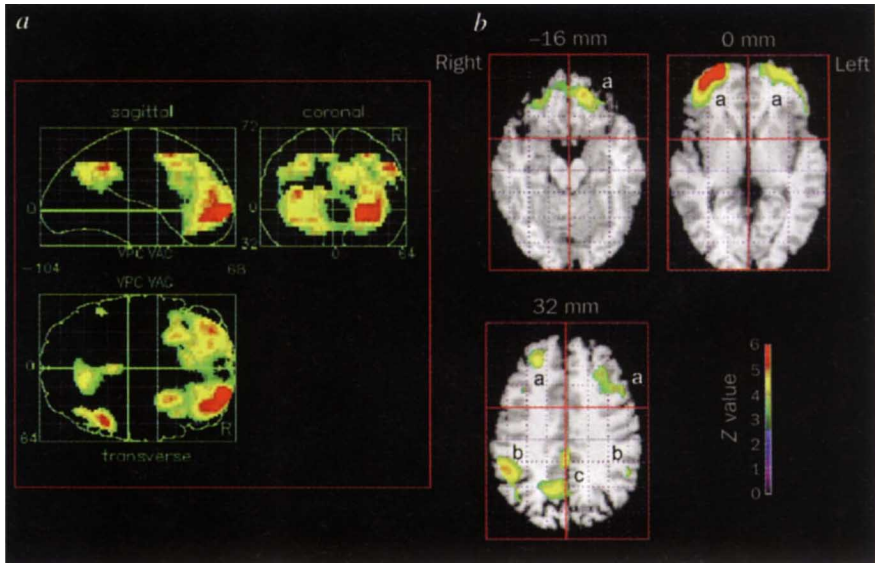

FIG. 2 Brain areas where activity showed a significant negative correlation with REM sleep. Functional PET results are displayed at threshold of $Z = 3.09$ ($P < 0.001$) by reference to the unit normal distribution. *a*, Projections within the stereotactic space[28]. *b*, Transverse sections where functional data are superimposed, for anatomical reference, upon a T1-weighted MRI scan normalized into stereotactic space. Section numbers refer to the distance from bicommissural plane. Methods as in Fig. 1: a, prefrontal cortex; b, parietal areas; c, precuneus and adjacent posterior cingulate cortex.

acteristics of dreams (temporal distortions, weakening of self-reflective control, amnesia on awakening[2]) might be related to the relative prefrontal deactivation. The suggested amygdalo-cortical activation could account for the perceptual components of dreaming. □

Received 17 April; accepted 8 July 1996.

1. Jones, B. E. *Neuroscience* **40,** 637–656 (1991).
2. Hobson, J. A. *The Dreaming Brain* (Basic books, New York, 1988).
3. Rechtschaffen, A. & Kales, A. A. *A Manual of Standardized Terminology, Techniques and Scoring System for Sleep Stages of Human Subjects* (Brain Information Service/Brain Research Institute, Los Angeles, 1968).
4. Hall, C. S. & van de Castle, R. L. *The Content Analysis of Dreams* (Appleton Century Crofts, New York, 1966).
5. Maquet, P. *et al. Brain Res.* **513,** 136–143 (1990).
6. Braun, A. R. *et al. Neurology* **42** (Suppl. 3), 182 (1992).
7. Buchsbaum, M. S. *et al. Life Sci.* **45,** 1349–1356 (1989).
8. Hong, C. C. H., Gillin, J. C., Dow, B. M., Wu, J. & Buchsbaum, M. S. *Sleep* **18,** 570–580 (1995).
9. Steriade, M., Jones, E. G. & Llinas, R. *Thalamic Oscillations and Signalling* (Wiley, New York, 1990).
10. Llinas, R. & Paré, D. *Neuroscience* **44,** 521–535 (1991).
11. Calvo, J. M., Badillo, S., Morales-Ramirez, M. & Palacios-Salas, P. *Brain Res.* **403,** 22–30 (1987).
12. Amaral, D. G., Price, J. L., Pitkänen, A. & Carmichael, S. T. in *The Amygdala. Neurobiological Aspects of Emotion, Memory, and Mental Dysfunction* (ed. Aggleton, J. P.) 1–66 (Wiley-Liss, New York, 1992).
13. Aggleton, J. P., Burton, M. J. & Passingham, R. E. *Brain Res.* **190,** 347–368 (1980).
14. Davis, M. *Annu. Rev. Neurosci.* **15,** 353–375 (1992).
15. Orem, J. & Keeling, J. in *Physiology in Sleep* (eds Orem, J. & Barnes, C. D.) 315–335 (Academic, London, 1980).
16. Amaral, D. G. & Price, J. L. *J. Comp. Neurol.* **230,** 465–496 (1984).
17. Bechara, A. *et al. Science* **269,** 1115–1118 (1995).
18. Gallagher, M. & Chiba, A. A. *Curr. Opin. Neurobiol.* **6,** 221–227 (1996).
19. Smith, C. *Behav. Brain Res.* **69,** 137–145 (1995).
20. Smith, C. & Lapp, L. *Sleep* **14,** 325–330 (1991).
21. Madsen, P. L. *et al. J. Cereb. Blood Flow Metab.* **11,** 502–507 (1991).
22. Aggleton, J. P. *Trends Neurosci.* **16,** 328–333 (1993).
23. Olson, C. R. & Musil, S. Y. *J. Comp. Neurol.* **324,** 237–260 (1992).
24. Fletcher, P. C. *et al. Brain* **118,** 401–416 (1995).
25. Paulesu, E., Frith, C. D. & Frackowiak, R. S. J. *Nature* **362,** 342–345 (1993).
26. Jonides, J. *et al. Nature* **363,** 623–625 (1993).
27. Devinsky, O. *et al. Brain* **118,** 279–306 (1995).
28. Friston, K. J. *et al. Human Brain Mapp.* **2,** 165–189 (1995).
29. Friston, K. J. *et al. Human Brain Mapp.* **2,** 189–210 (1995).

ACKNOWLEDGEMENTS. We thank R. S. J. Frackowiak and K. J. Friston for providing the statistical parametric mapping software, P. Hawotte and M. Piérrard for (nocturnal) technical assistance, G. Hartstein for checking the manuscript, and S. Fuchs and V. Delvaux for help with subject selection. P.M. is research associate at the Fonds National de la Recherche Scientifique de Belgique (FNRS). This research was supported by FNRS grants, by the European Sleep Research Society-Synthélabo Research Grant 1994 and the Queen Elisabeth Medical Foundation.

CORRESPONDENCE and requests for materials should be addressed to P.M. (e-mail: maquet@pet.crc.ulg.ac.be).

Induction of cell death by endogenous nerve growth factor through its p75 receptor

José María Frade, Alfredo Rodríguez-Tébar* & Yves-Alain Barde

Max-Planck Institute for Psychiatry, Department of Neurobiochemistry, 82152 Planegg-Martinsried, Germany
* Cajal Institute, CSIC, Doctor Arce 37, E-28002 Madrid, Spain

During development, neuronal survival is regulated by the limited availability of neurotrophins, which are proteins of the nerve growth factor (NGF) family. Activation of specific *trk* tyrosine kinase receptors by the neurotrophins blocks programmed cell death. The *trk*A-specific ligand NGF has also been shown to activate the non-tyrosine kinase receptor p75, a member of the tumour necrosis factor (TNF) receptor and Fas (APO-1/CD95) family. Here we report that, early in development, endogenous NGF causes the death of retinal neurons that express p75 but not *trk*A. These results indicate that, as with cells of the immune system, the death of neurons in the central nervous system can also be induced by ligands, and that the effect of NGF on cell fate depends on the type of receptor expressed by developing neurons.

The elimination of neurons has long been recognized as an integral part of normal development. In vertebrates, this phenomenon is particularly well documented during the time corresponding to the innervation of target cells[1], and is easily monitored as net cell numbers decrease over time. During this period, programmed cell death can be prevented by the administration of exogenous neurotrophins, or increased by neutralizing the neurotrophins with antibodies or by deleting their genes[2]. Prevention of cell death involves tyrosine kinase receptors of the *trk* family, as the deletion of the genes coding for these receptors generates phenotypes similar to those resulting from ligand elimination[3]. In addition, cell death can also be observed in the nervous system before innervation of the target cells. Soon after leaving the cell cycle, many neurons die, as has been shown in the cerebral cortex[4], and in the worm *Caenorhabditis elegans*.[5] Here we consider the regulation of this early form of neuronal death.

In the absence of *trk*A, NGF can signal in non-transformed cells through the neurotrophin receptor p75, as shown by the nuclear translocation of the transcription activator NF-κB[6]. To examine the relevance of p75 activation by NGF *in vivo*, we investigated the consequences of NGF removal on the development of the chick retina. Previous *in situ* hybridization studies[7] have demonstrated the presence of p75 messenger RNA as early as embryonic day 4 (E4), and staining of E6 retinal sections with antibodies to chick p75 confirmed the presence of this receptor mostly in the central retina, but also on scattered cells (data not shown). The *NGF* gene is expressed as early as E4, but the *trkA* gene is expressed only later in development (Fig. 1). Cell death is widespread in the dorsal part of the chick retina as early as E4 (ref. 8), before innervation of the tectum begins, and TUNEL staining, which detects DNA fragments on tissue sections, revealed a pattern corresponding to that of p75 expression (Fig. 2*e*). Double labelling with p75 antibodies showed that 95% of the TUNEL-positive cells were also p75-positive (94 cells counted). To test the possibility that endogenous NGF causes cell death, cells secreting an anti-NGF monoclonal antibody[9] were applied onto chick embryos at E2.5. When examined at E6, the retinae of embryos treated with anti-NGF antibodies showed a remarkable reduction in the number of TUNEL-positive cells when compared with those of control embryos (Fig. 2; compare *c* with *d*, and *e* with *f*). To quantify the reduction in cell death resulting from the administration of anti-NGF antibodies, soluble nucleosomes were measured in retinal extracts by using an immunoassay combining anti-DNA and anti-histone antibodies[10]. A marked reduction was observed at E6 (Table 1), and in three embryos, cell death was reduced by as much as 80%. Similar effects were observed with sheep anti-NGF polyclonal antibodies, but hybridoma cells producing an anti-NT-3 antibody had no

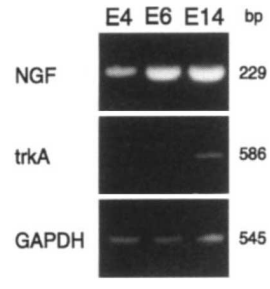

FIG. 1 *NGF* and *trkA* gene expression in the developing chick retina.